# Progress on the Structural and Mechanical Design of the Giant Magellan Telescope

Michael Sheehan*[a], Steve Gunnels[b], Charles Hull[a] , Jonathan Kern[a], Carey Smith[a], Matt Johns[a], Stephen Shectman[a]
[a]GMTO Corp., 251 S. Lake Ave. Pasadena, CA USA 91101;
[b]Paragon Engineering, 2277 Joy Lane, Westcliffe, CO USA 81252

## ABSTRACT

The Giant Magellan Telescope (GMT), one of several next generation Extremely Large Telescopes (ELTs), is a 25.4 meter diameter altitude over azimuth design set to be built at the summit of Cerro Campanas at the Las Campanas Observatory in Chile. The primary mirror consists of 7 individual 8.4 meter diameter segments resulting in an equivalent collecting area of a 21.5 meter diameter single mirror. The telescope structure, optics and instrumentation has a rotating mass of approximately 1250 metric tons and stands approximately 40 meters tall. This paper reports the results of our ongoing preliminary design and development of the GMT structure and its major mechanical and opto-mechanical components. A major recent redesign of the Gregorian Instrument Rotator (GIR) resulted in significant changes to the telescope structure and several mechanisms. Design trade studies of various aspects of the main structure, hydrostatic bearing system, main axes drives, M2 positioner, M3 subsystem and the corrector-ADC subsystem have refined the preliminary design in these areas.

**Keywords:** Giant Magellan Telescope, telescope structure

## 1. INTRODUCTION

The GMT is an altitude over azimuth design consisting of a primary mirror with 7 individual 8.4 meter diameter segments and a secondary mirror consisting of 7 segments, each approximately 1 meter in diameter set in a Gregorian optical configuration. The elevation axis is 25.5 meters above grade level. Structural elements making up this distance include a 12.4 meter tall reinforced concrete pier, a 0.8 meter tall azimuth track assembly, a 1.6 meter tall azimuth disk assembly (to the telescope floor) and an elevation runner bearing radius of 10.5 meters. The telescope has a swept volume radius of 25.5 meters centered at the intersection of the optical axis and the elevation axis, 11 meters above the telescope floor. The telescope, including all optics, instruments and azimuth track has an estimated total mass of 1400 metric tons. Other papers describing aspects of the structural design of the GMT have been written by Gunnels [2,3]. An overview of the GMT project is presented by Johns [4].

A significant departure from the GMT conceptual design is the new Gregorian Instrument Rotator (GIR). This new GIR provides increased flexibility by incorporating several large and several small instruments ready to be cycled into and out of the optical beam on demand to reconfigure the telescope in a relatively quick and efficient way. The new GIR accommodates 45 metric tons of science instruments at the direct Gregorian level, each in an actuated instrument support frame that translates the instrument from a parked position to the observing position. The GIR also accommodates 11.1 metric tons of fixed science instruments in 3 locations at the folded port level, above the top disk of the GIR. The optical beam is fed to these fixed instruments by a deployable tertiary mirror (M3 subsystem). Additional instrumentation locations include a gravity invariant station on the azimuth disk with the optical beam transmitted to the instrument by an optical relay or by fiber, 2 gravity invariant auxiliary port instrument stations at the elevation axis intersection with the C-rings (see section 3.2 below) and a fixed instrument station on the fixed instrument platform.

Another significant feature of the telescope design is that the elevation axis is now located in the folded port plane as defined by the rotation of the optical axis by the tertiary mirror. This feature of the telescope resulted largely from aspects of the new GIR design and increased instrument mass allocation. In order to balance the elevation structure with this added mass (and keep the elevation axis location unchanged), much of the elevation axis mass moved upward to compensate for the added GIR and instrument mass below the elevation axis. The result had the folded port plane very close to the elevation axis and only a small amount of additional counterbalance mass was needed to align these features.

*msheehan@gmto.org phone 626 204-0524; fax 1 626 204-0504; www.gmto.org

The telescope includes interchangeable adaptive secondary mirror and a fast-steering secondary mirror top ends. The fast-steering secondary mirror top end is intended for commissioning purposes and for use when the adaptive secondary mirror top end is out for service and/or maintenance. An efficient change capability for these top end systems is being developed to minimize operational downtime.

## 2. OVERVIEW OF THE STRUCTURAL DESIGN

An overall view of the GMT is shown in Figure 1. The main structural components include both long-span, slender space-frame elements and large, plated monocoque structures as appropriate to maximize the static and dynamic performance of the telescope and to provide support for the optics, opto-mechanical subsystems and instruments. The azimuth structure is supported by an azimuth track attached to the top of a 12 meter tall reinforced concrete pier. The mechanical interface between the azimuth structure and the track is through sets of vertical and radial hydrostatic bearings. The azimuth structure includes 4 pedestals, each directly above a set of azimuth bearings, providing direct support of the elevation structure. The interface between the elevation and azimuth structures is again through sets of radial and lateral hydrostatic bearings. This structural configuration provides a high stiffness load path between the elevation structure and the pier. The backbone of the elevation structure consists of 2 large C-rings. The outer surfaces of the C-rings include the runner bearing surfaces for the elevation axis. The C-rings are structurally joined by an open space frame spanning between the inner faces of each C-ring along their perimeters. The wide separation of the C-rings and rigidity of the bracing structure results in high lateral stiffness of the lower end of the elevation structure. The 7 primary mirror segment cells each include continuous top and bottom plates separated a distance of approximately 2 meters. The cells are joined together in the telescope structure by bolted joints along their top and bottom plates creating 2 very rigid, braced diaphragms. The cells are additionally connected through a cell connector frame (CCF) consisting of a central hexagonal hub and 6 spokes. The CCF provides continuity of load paths through the cell structures and it also provides a structural interface to the C-rings below and the main truss, above. The main truss is a braced hexapod with each tripod leg configured in a high stiffness X-configuration. The cross-over is oriented to eliminate obscuration of light to the 6 outer segments of the primary mirror. Weak axis bracing is provided by 2 struts per tripod leg. The top frame consists of a hexagonal box-beam weldment attached to the top of the main truss legs. The top frame provides a compact interface with the secondary mirror positioning system and efficient placement of the secondary mirror assemblies. Mirror covers are provided to protect the primary mirror segments during non-operational periods.

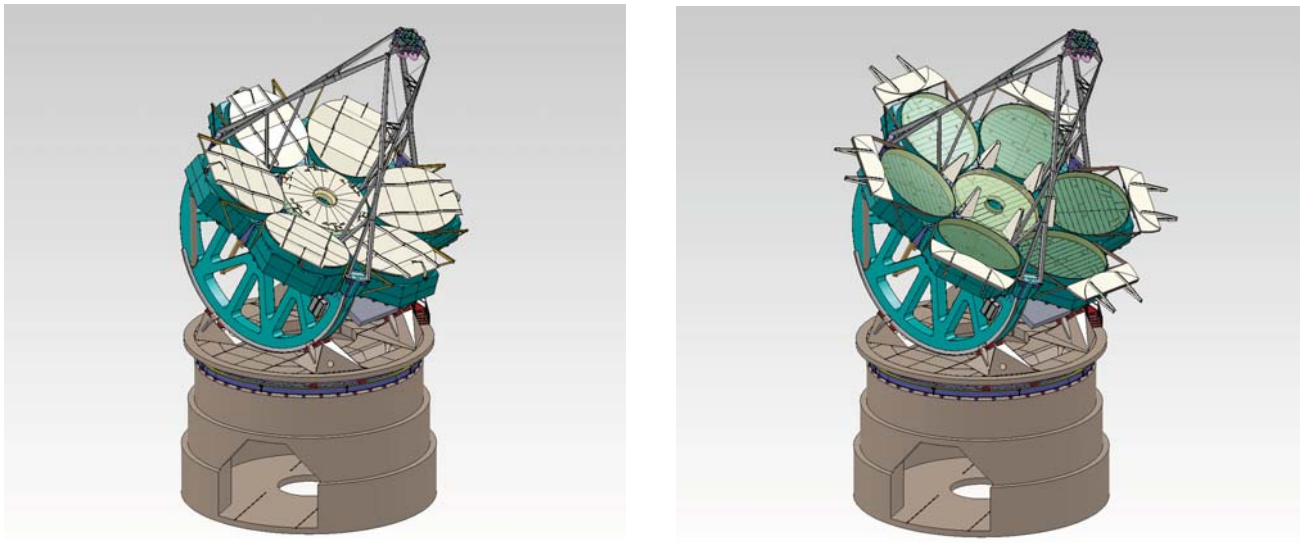

Figure 1. Overall view of the GMT structure and telescope pier with mirror covers closed (left) and open (right)

# 3. OPTICAL SUPPORT STRUCTURE (OSS)

## 3.1 General Overview of the OSS

The OSS generally consists of the global structure, primary, secondary and tertiary optics, wide field corrector and atmospheric dispersion compensator, mechanical subsystems and components that move in the elevation plane. The OSS provides interfaces for telescope instruments and adaptive optics subsystems.

## 3.2 C-Ring Assembly

The C-ring assembly consists of 2 large, parallel semicircular braced C-rings separated a distance of approximately 11.6 meters, center-to-center and connected at their outer perimeters by open space frame C-ring bracing. The C-ring assembly also includes braced struts that provide support for the outer mirror cells and vertical posts attached to the C-ring bracing that provide axial support for the GIR. The C-ring assembly is shown in Figure 2.

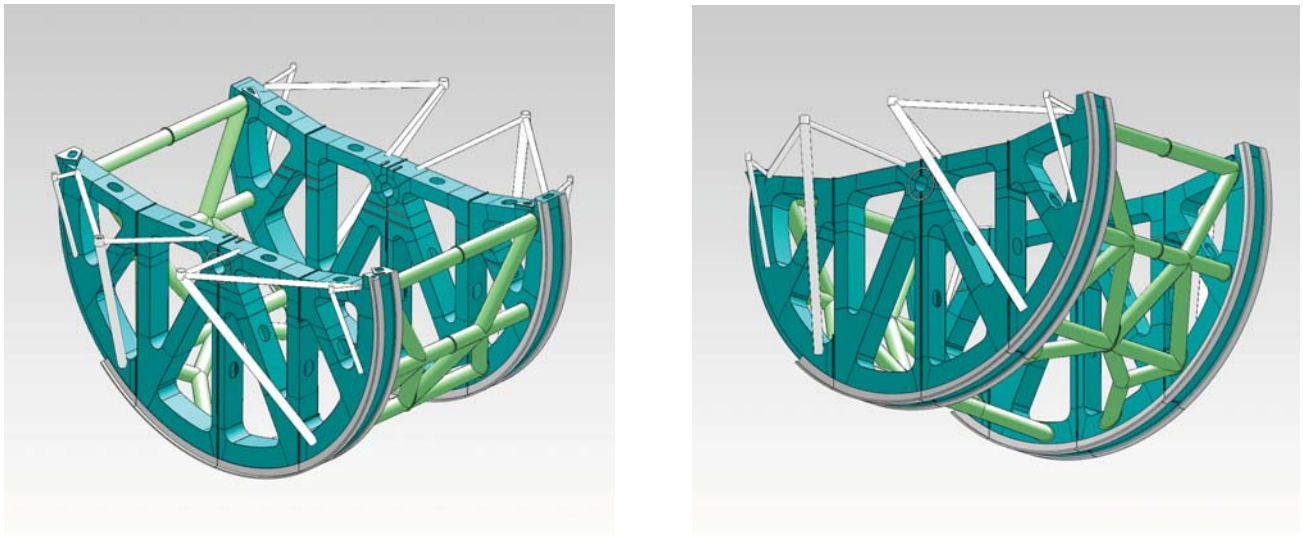

Figure 2. C-Ring assembly

The 2 C-rings are large monocoque structures, each constructed in 4 separate pieces that are field bolted together during final assembly. The 4 pieces of the each C-ring are shown in Figure 3. Except for the runner bearings, the C-rings are constructed nominally from 12.5mm thick plate throughout. The outer surface of the each C-ring includes 2 parallel runner bearing surfaces on a 10.5 meter radius and spaced 1.3 meters apart that interface with two rows of elevation hydrostatic bearing pads. A cross-section through this area of the C-ring is shown in Figure 4. The structure of the runner bearings was optimized by analysis of the runner bearing distortion and stress as a result of the forces applied to the C-ring from the hydrostatic bearing pads. Bearing pad forces at and between the C-ring spokes were considered. We also looked at the relative performance aspects of a 4 pad local group and a 6 pad local group (see section 7.2 for details). The optimized design includes 80 mm thick and 420 mm wide runner bearing plates and a 4 HBS pad local group. The maximum relative distortion between the runner bearing and HBS pad surface under normal operational conditions is calculated to be ±8.7 microns which can easily be accommodated in the nominal 65 micron oil film gap produced by the hydrostatic bearings. The outer ring also provides interfaces for the elevation drives, encoding system, locking pins and end-of-travel stops. The C-rings provide a structural interface with the primary mirror structure assembly along their top surfaces and a fixed instrument platform (IP) approximately 2 meters below the bottom of the on-axis primary mirror segment cell.

Additional support for the outer mirror cells is provided by braced struts that span between the bottom of the mirror cells and the C-ring. These struts act to provide a stable support for the mirror cells during installation and removal from the telescope with fasteners at the main structural joints removed but they also add significant structural stiffness under static and dynamic loading. Bipod, tripod and quadrapod configurations for these braces are being considered in the preliminary design. A design with tripods and bipods for the 4 lateral cells and is shown in Figure 2.

The C-ring brace forms the rigid structural tie between the 2 parallel C-rings. It is a space-frame consisting of tubular members oriented along the outer perimeter of the C-rings. The frame elements are nominally 0.75 meter diameter circular tubes with a nominal wall thickness of 12.5 mm. This C-ring and C-ring brace assembly has very high lateral stiffness and is key to providing good dynamic performance of the OSS.

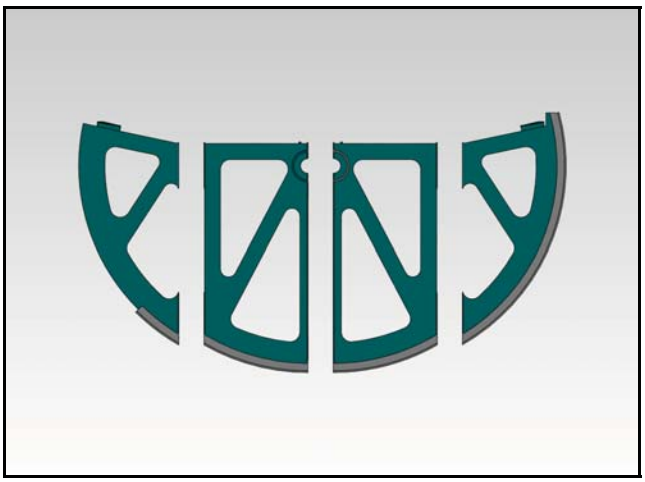

Figure 3. The 4 Individual C-Ring parts

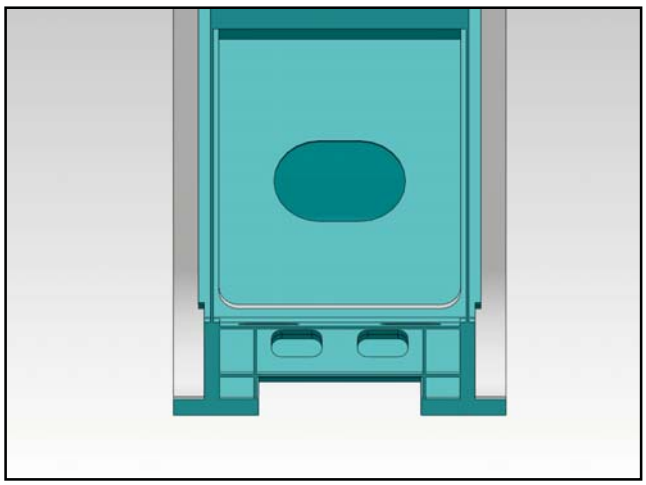

Figure 4. C-Ring cross-section through the runner bearings

### 3.3 Primary Mirror Structure Assembly

The primary mirror structure assembly includes the 7 primary mirror cells and the cell connector frame (CCF). The assembly is shown in Figure 5 below.

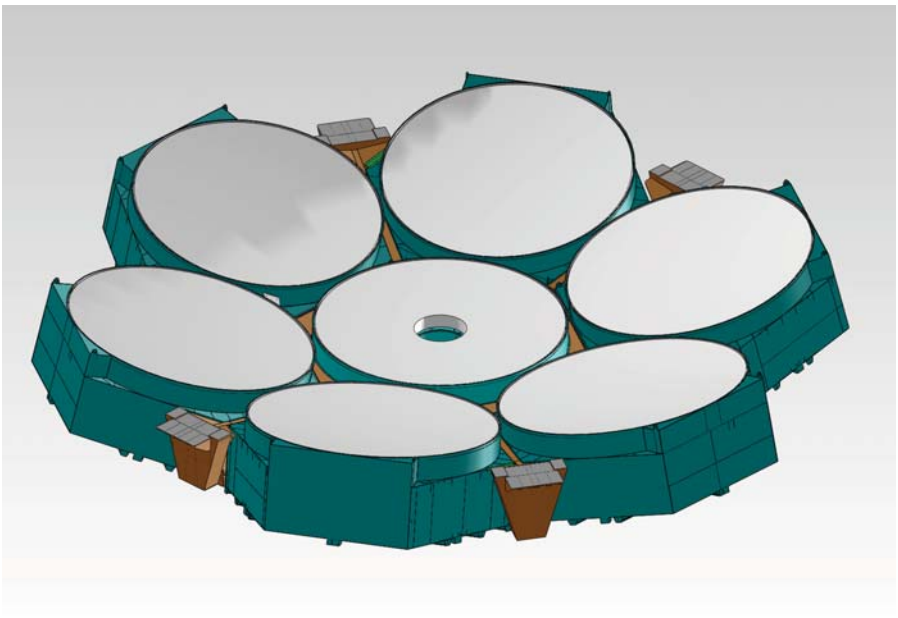

Figure 5. Primary Mirror Structure Assembly

There are 6 identical off-axis primary mirror segment cells and these cells are interchangeable at any off-axis segment location. Each cell structure is a continuous braced hexagonal weldment and includes heavily stiffened top and bottom plates and a central braced plane truss. The top plate stiffeners and braced plane truss provide a relatively rigid interface

for the mirror support actuators, reducing the travel required for the mirror support actuators during operation. The off-axis mirror cell structure and a cross section showing the stiffened top and bottom plates and global braced plane truss is shown in Figure 6, below. The lateral distance between the vertical sidewalls is approximately 9 meters and the vertical distance between the top and bottom plates is approximately 2 meters. The top and bottom plates of each cell act as elements of continuous membrane diaphragms when connected to other cells and the CCF. This diaphragm action and the 2 meter separation between the diaphragms contribute significantly to the bending stiffness of the mirror cell and CCF assembly. The 2 meter head-room also provides generous space within the mirror cells for maintenance of the primary mirror segment support and temperature control subsystems.

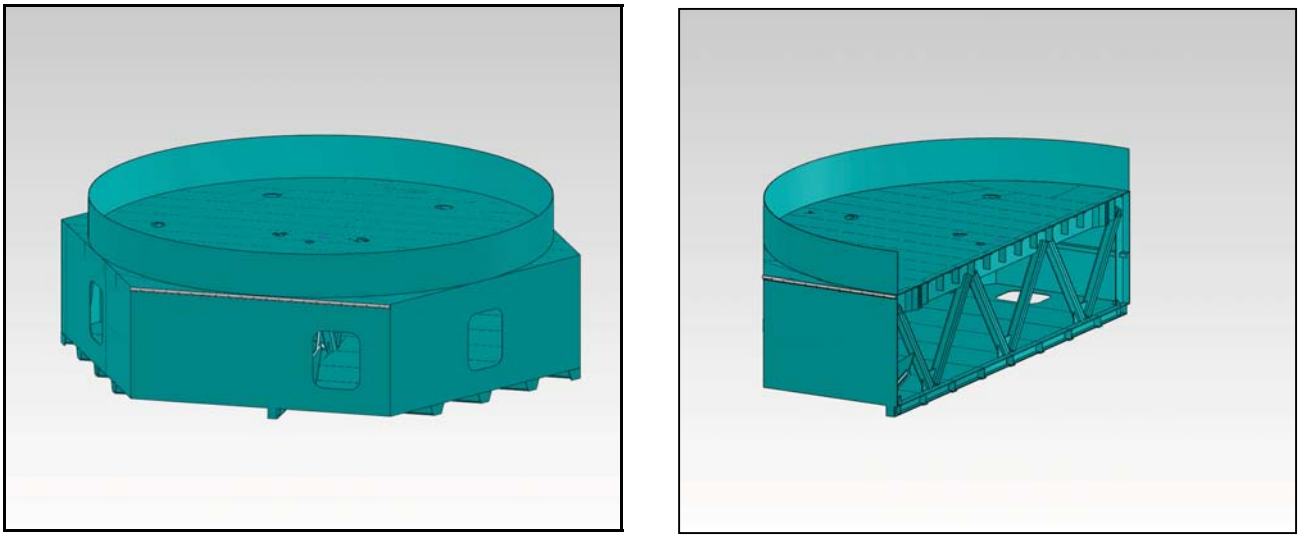

Figure 6. Off-axis primary mirror cell structure and cross-sectional view

The mirror cells provide structural interfaces for the primary mirror static support springs, mirror support actuators, hardpoint hexapod positioning system, mirror temperature control system and the power, cooling fluid, communications fiber and cabling and compressed air services. The cell assemblies are readily removable from the telescope for recoating the primary mirror segments. All mirror cells have deployable mirror covers. Infrastructure for in-situ washing of the primary mirror segments is being considered in the preliminary design.

The on-axis mirror cell is circular in construction and has all of the features described for the off-axis segments. The central cell also provides an interface for a large wide field corrector and atmospheric dispersion compensator (ADC) that is inserted into and retracted from the optical beam depending upon the observation mode employed.

The cell connector frame (CCF) is a structural framework consisting of a central hexagonal hub and 6 radial spokes. The elements of the hub and spokes are box beams with trapezoidal cross-section that act as structural in-fill between the primary mirror segment cells and provide continuity of the diaphragm based load path through the top and bottom plates of the mirror cell structures. The CCF acts as the structural interface between the primary mirror cell assemblies and the C-ring assembly and it also provides a stiff interface with the main truss. CCF spokes that interface with the main truss include torsional bracing features that improve the modal performance of the main truss and top frame. The CCF is shown in Figure 7, below.

### 3.4 Main Truss and Top Frame Assembly

The main truss and top frame assembly consists of the three main truss subassemblies (three leg pairs), the top frame weldment and the mechanisms used to join these structures together.

The main truss is a braced hexapod that provides a high stiffness interface to the top frame for all translational and rotational degrees of freedom. This is a result of the three bipods at the top end of the hexapod truss providing two stiff degrees of freedom to each end of the triangular M2 frame. The cross-over of each tripod leg is oriented such that the truss does not obscure light to the off-axis primary mirror segments. Obscuration of the on-axis segment is minimized.

The main truss spans between 3 of the 6 CCF spokes to the top frame. The truss structure consists of slender, long-span box beams with rectangular or parallelogram-shaped cross-sections and relatively thin walls. Secondary bracing elements in the upper truss planes are provided where necessary to increase leg local resonant frequencies and thus improve the dynamic performance of the truss. A sketch of the main truss is given in Figure 8.

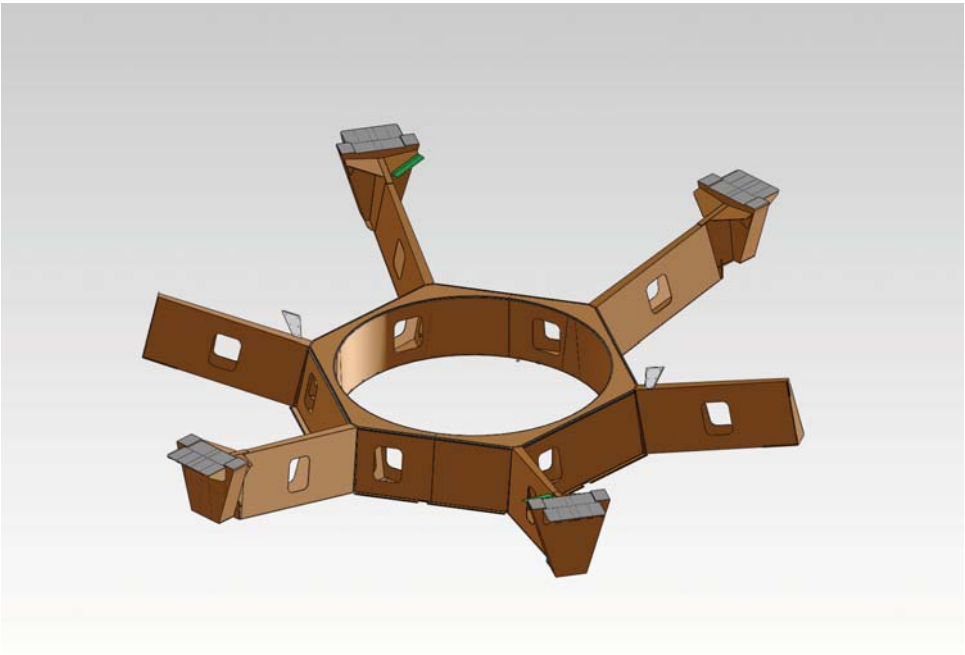

Figure 7. Cell Connector Frame (CCF)

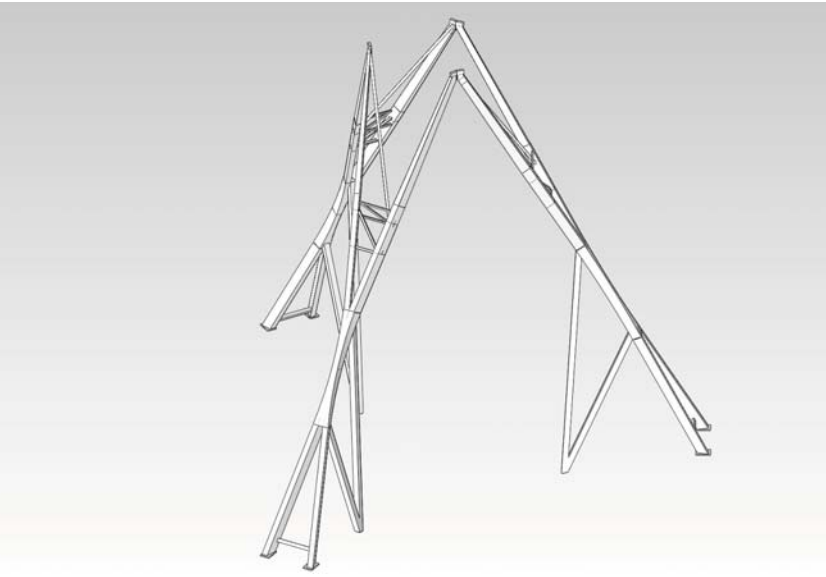

Figure 8. Main truss

Performance of the telescope in the wind environment as reported by Kan[8] indicated that the main truss 2nd and 3rd fore/aft bending modes contributed significantly to focal plane image motion. In light of these results, GMT performed studies investigating the feasibility of using advanced composite structures for parts of the main truss to improve its inherent dynamic performance. We also investigated the feasibility of adding either passive or active damping features to the main truss. No significant improvement in telescope performance was evident by use of advanced composite materials and the current preliminary truss design is all steel in construction. The addition of damping to the main truss, either passive or active in nature, tends to reduce focal plane image motion in a strong wind environment by approximately 20%. More information on the GMT damping studies is presented by Glaese[7].

The top frame is a continuous box-beam weldment spanning the top nodes of the main truss. The frame provides support for the secondary mirror positioning system, a fast steering secondary mirror system or an adaptive secondary mirror system and their associated electronics and services. To enhance the local modal performance of the top frame, the secondary mirror positioning system actuators are nested within the structural elements of the top frame. This compact arrangement allows full motion capability of the positioning system and keeps the center of mass of the M2 subsystems as close as possible to the top frame structure. The compact nature of this assembly also allows the possibility of mounting secondary mirror system electronics on the top frame in areas where they are easily accessible for service and repair. A sketch of the top frame is given in Figure 9.

Two top frame assemblies will be constructed; one for the adaptive secondary mirror segments and one for the fast-steering secondary mirror segments. Switching between one frame and the other will require the design of the attachment of the top frame to the main truss to be easily released and reattached. Several options are being considered for this including various bolted joints and several types of automatic or semi-automatic latches. Alignment features will be provided to assure repeatable attachment of the top frame assemblies.

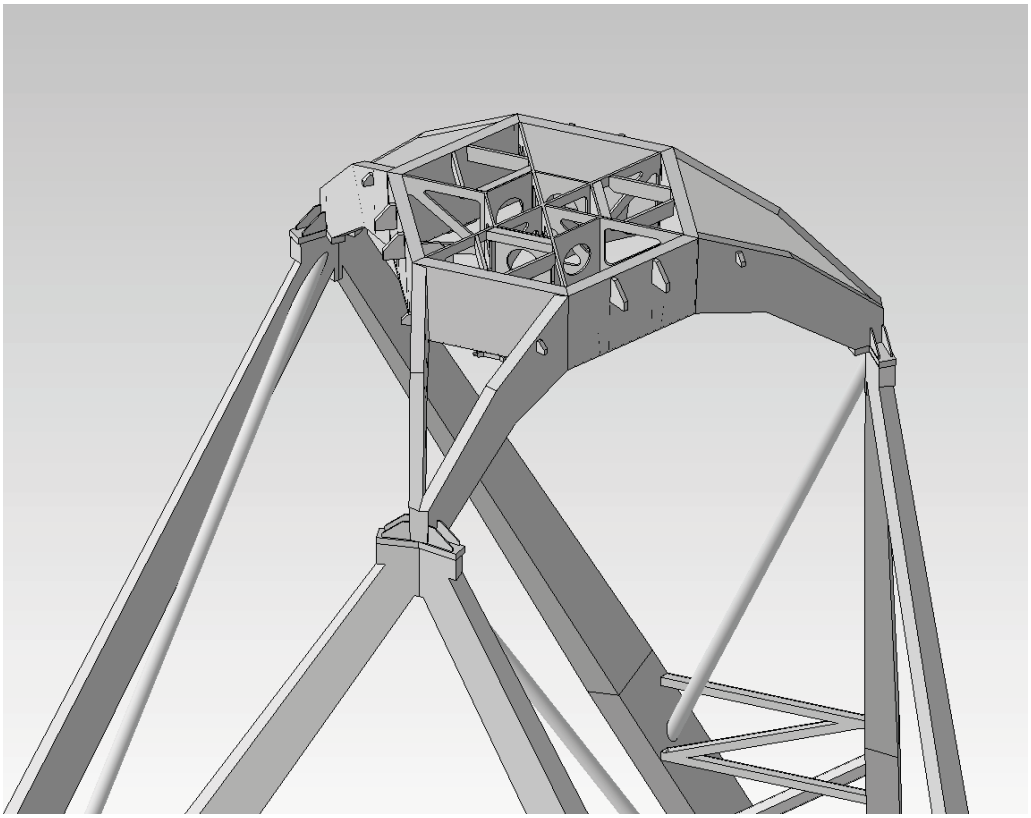

Figure 9. Top Frame Structure

### 3.5 OSS Mass summary

A summary of the mass of the major OSS components is given in Table 1, below.

Table 1. OSS Mass summary

| System | Subsystem | Mass (kg) |
|---|---|---|
| Telescope Structure | C-Rings | 238730 |
| | Cell Connector Frame | 56444 |
| | M1 Cell Structure | 195358 |
| | Top End Frame | 3208 |
| | Main Truss | 20442 |
| | Instrument Platform Structure | 61508 |
| | Access Platforms | 9180 |
| | GIR Structure & Mechanical | 60700 |
| Primary Mirror Supports and Vents | Primary Mirror Segments | 116813 |
| | M1 Supports & Vents | 24726 |
| Opto-Mechanical Subsystems | Corrector-ADC | 3586 |
| | M3 Subsystem | 1300 |
| | AcWFS Subsystem | 700 |
| | AO Subsystems | 20780 |
| | GIS Pick-off Mirror | 700 |
| Instruments | Folded Port Instruments | 11130 |
| | Direct Gregorian Instruments | 45000 |
| | Instrument Platform Instruments | 7000 |
| | Auxiliary Port Instruments | 3000 |
| Services | Cable Wraps | 2400 |
| | System Services | 12406 |
| | M1 Covers | 9072 |
| | Counterweights | 24333 |
| | Misc Mechanical | 895 |
| | **Total** | **929411** |

## 4. AZIMUTH STRUCTURE

### 4.1 Azimuth Disk

The azimuth disk consists of a set of 8 braced, plated, monocoque structural elements, field bolted together at final assembly and designed to provide a direct load path between the OSS structure and the azimuth track & pier. It provides support for the elevation and azimuth hydrostatic bearings and the elevation and azimuth drives. The assembly includes features that optimize the stiffness of the vertical and lateral structural load paths, but at the same time provides flexibility for the azimuth disk to absorb relative vertical motion resulting from flatness irregularities of the azimuth track. The total mass of the azimuth disk assembly is approximately 325 metric tons. A sketch of the azimuth disk assembly is given in figure 10, below.

### 4.2 Azimuth Track Assembly

The azimuth track is a structure that provides a vertical and lateral interface between the telescope structure and the reinforced concrete pier. It consists of 8 individual sections, field bolted together at final assembly. The track is a circular ring with an inner diameter of 16.8 meters and an outer diameter of 21.2 meters. A runner bearing surface is provided along the inner radius to interface with the azimuth radial hydrostatic bearing pads. The top surface of the track includes 2 concentric runner bearing surfaces that intersect with 2 radial rows of azimuth vertical hydrostatic bearing pads. These runner bearing surfaces are centered on 17.2 meter and 20.8 meter diameters.

The track sections are bolted together at flange joints and the assembly is attached to the top of the telescope pier at discrete locations. Spacing of the track to pier joints is designed such that the vertical hydrostatic bearings all cross pier attachment points at the same time resulting only in a small, global vertical motion of the telescope as the bearing pads cross synchronously from the more flexible to more rigid areas of the track.

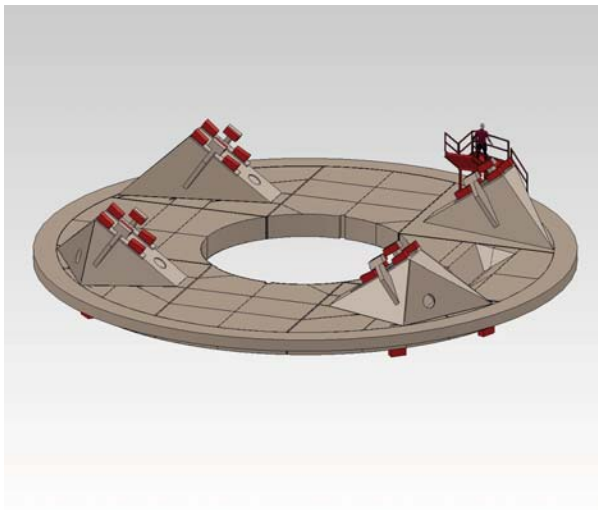

Figure 10. Azimuth disk assembly

A sketch of the azimuth track assembly is shown in Figure 11. Each of the 8 track sections has a mass of approximately 15 metric tons. The azimuth track assembly also provides interfaces for the HBS vertical and radial pads and oil collection system, the azimuth drive and azimuth position encoding system.

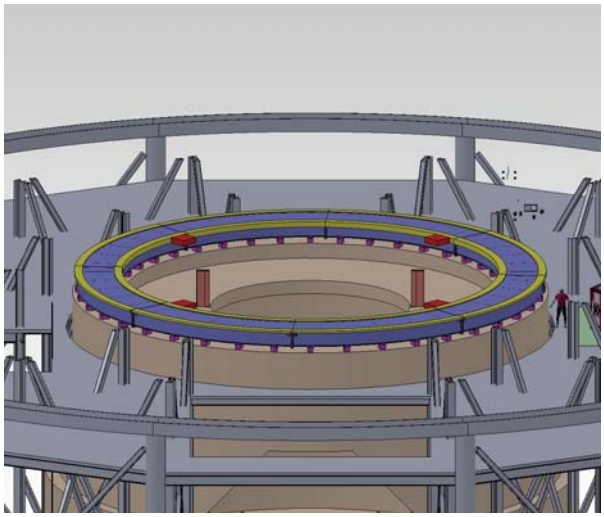

Figure 11. Azimuth track assembly

# 5. GREGORIAN INSTRUMENT ROTATOR (GIR)

## 5.1 GIR Overview

The GIR design had been recently revised to provide access to the Gregorian focus within the 9 meter diameter and 6.5 meter long cylindrical GIR structure for 4 large instruments with a total instrument mass of 45 metric tons. The instruments are mounted within frames and attached to the GIR structure through rails, allowing the instruments to be moved from a parked position near the outer radius to an operational position at the center of the GIR. The GIR also includes fixed instrument mounting locations on the top disk as well as interfaces for deployable subsystems including a tertiary mirror (M3 subsystem), pick-off mirror for a fiber feed to a gravity invariant instrument station on the azimuth disk and a ground layer adaptive optics dichroic and wavefront sensor subsystem. The GIR also provides an interface for the active optics guiding and wavefront sensing subsystem and an adaptive optics phasing camera. An overall view of this design is shown in Figure 12 with the conceptual representations of GMT instruments in the instrument bays. More information on the adaptive optics aspects of the telescope design are provided by Bouchez [5].

The GIR is rigidly mounted to the telescope structure through a series of precision track rollers and friction drives attached to the Instrument Platform at the GIR top disk and to the C-ring braces at the bottom disk. Other mechanical components include a dynamic counterbalancing system to maintain the center of mass of the GIR at its center of rotation, locking pins, position encoding system and a cable wrap.

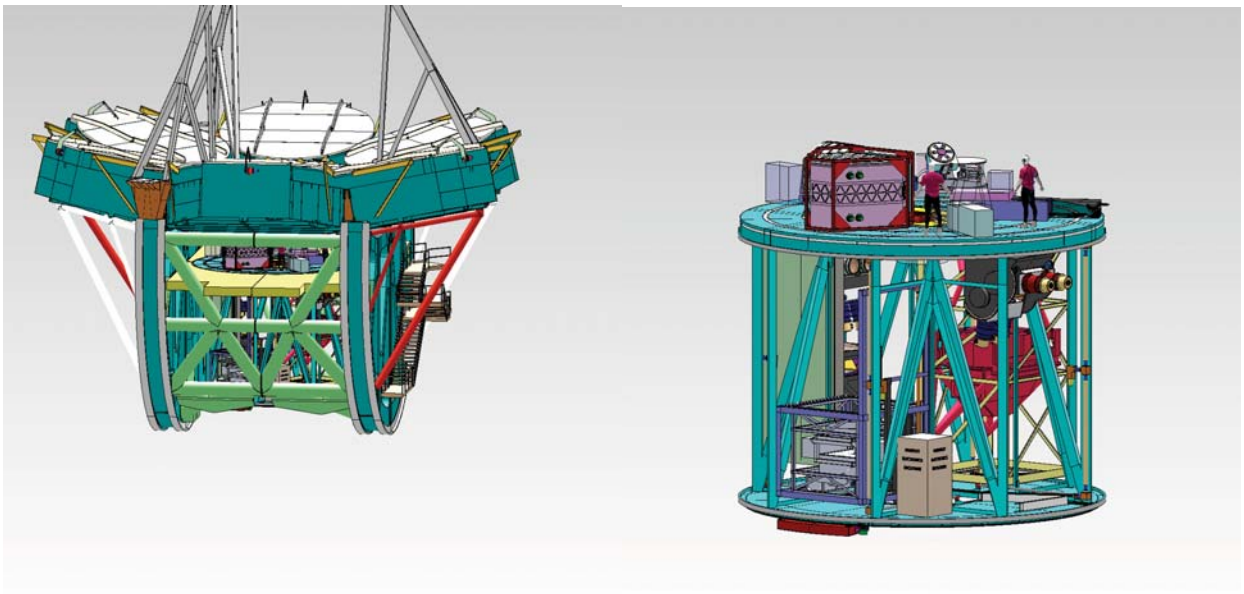

Figure 12. Overall view of the GIR within the telescope structure (left) and the populated assembly (right)

### 5.2 GIR Structure

The main structural elements of the GIR include the upper disk and lower disk weldments and 4 sets of corner braces, all constructed from low-carbon steel plate varying from 12.5mm to 50mm in thickness. The upper disk weldment is a short cylinder with integral top and bottom plates for added stiffness. The outer rings of the disks are constructed from flame hardened and ground, high strength 4140 steel. Axial and lateral loads from the 4 movable instruments are transferred to the upper disk through THK LM guide rails mounted on the bottom surface of the upper disk. The corner braces serve to stiffen the load path through the upper disk to the GIR interface with the telescope structure and to provide continuity between the upper and lower GIR disks. Instrument guide rails along the lower disk react lateral load only. These forces are transmitted directly through the lower disk to the lateral GIR/Telescope interface.

### 5.3 GIR Mechanical Subsystems

Several types of bearing mechanisms have been considered for load transfer between the GIR and the telescope structure. These include conventional rolling element bearings, hydrostatic bearings, linear bearings/guides and high capacity precision track rollers. An evaluation of these different systems was made using criteria including load capacity, complexity, availability, reliability, maintainability, performance and cost. The most favorable candidate solution is a set of precision track rollers and the RBC CRBY9 Yoke Roller was selected for the preliminary design. The bearing system consists of 8 axial 10 radial rollers on the upper disk and 10 radial rollers on the lower disk.

The upper disk transfers axial and lateral load to the Instrument Platform and C-ring bracing structure through the RBC rollers in contact with the 2 machined surfaces along the perimeter of the disk. The lower disk transfers lateral load only through radially oriented RBC rollers fixed to the C-ring bracing structure.

A subscale test was conducted to assess performance and life characteristics of the RBC rollers and track. The roller was loaded to produce the maximum Hertz stress and subjected to 2.7 million cycles with no damage to the track or roller (50 years of service is equal to 1.5 million cycles). Conclusions from this testing indicate that the rollers and track will have adequate life if lubricated with grease or oil and will not have adequate life without lubrication (even with a conical roller). It is suggested that, even with a conical roller, micro-scrubbing causes a stress condition that fatigues the track and (later) the roller. Lubrication appears to not only keep fatigue from occurring but allows operation with surfaces that were previously subject to fatigue damage (due to operation without lubrication). Starting and rolling coefficients of

friction for each roller will be approximately 0.0030 and 0.0024 at the radius of the track. Although acceptable, this friction can be reduced considerably by purchasing the rollers with internal thrust bearings. Measurements indicated the total friction with thrust bearings installed might be about half these values.

GIR drive options include the use of linear motors, gear drives and friction drives. All of these drive options can be made to work adequately. With the current bearing design requiring a machined surface on the outer radius of the upper disk, a friction drive was selected for the preliminary design. The 2 friction drives each consist of a 200 mm diameter drive roller mounted to a roller housing through a pair of high capacity tapered roller bearings and directly coupled to a servo motor. The housing is attached to the telescope structure through blade flexures with high tangential stiffness and low radial stiffness. Each roller is preloaded against the drive track with a force of approximately 85 kN.

Additional mechanical subsystems for the GIR include locking pins, which are necessary with the use of a friction drive system and a movable counterweight system to keep the GIR center of mass on its rotational axis. A cable wrap will be used to transfer services from the OSS to the GIR and local utility transfer systems will be employed to manage services between the GIR structure and the instruments.

## 6. OPTO-MECHANICAL SUBSYSTEMS

Preliminary design of the major opto-mechanical subsystems has just begun so few design details have been established to date. The sections below highlight some of the key functional and performance criteria for these subsystems.

### 6.1 M3 Subsystem

The M3 Subsystem consists of an elliptical flat mirror (M3) deployed to the GMT reference optical axis (ROA) to direct the optical beam to one of several fixed instrument stations at the folded port level of the GIR. The subsystem includes a deployment mechanism to move the M3 mirror and support system from its parked position within a protective enclosure to the ROA. It also includes slow tip, tilt and piston articulation of the M3 Mirror to compensate for beam motion due to structural flexure and thermal expansion and contraction.

### 6.2 Corrector-ADC

The corrector-ADC subsystem provides image quality improvement of the nominal Gregorian focal surface over a 20 arc minute field of view. The corrector-ADC Subsystem also provides correction of atmospheric dispersion from zenith to an elevation angle of 40 degrees. The subsystem deploys into the optical beam when in use. All components of the corrector-ADC Subsystem are contained within and mounted to the central M1 cell weldment with the exception of a field lens, which is mounted just above the Gregorian focus. Views of the conceptual design of the corrector-ADC in its parked and deployed positions are shown in Figure 13.

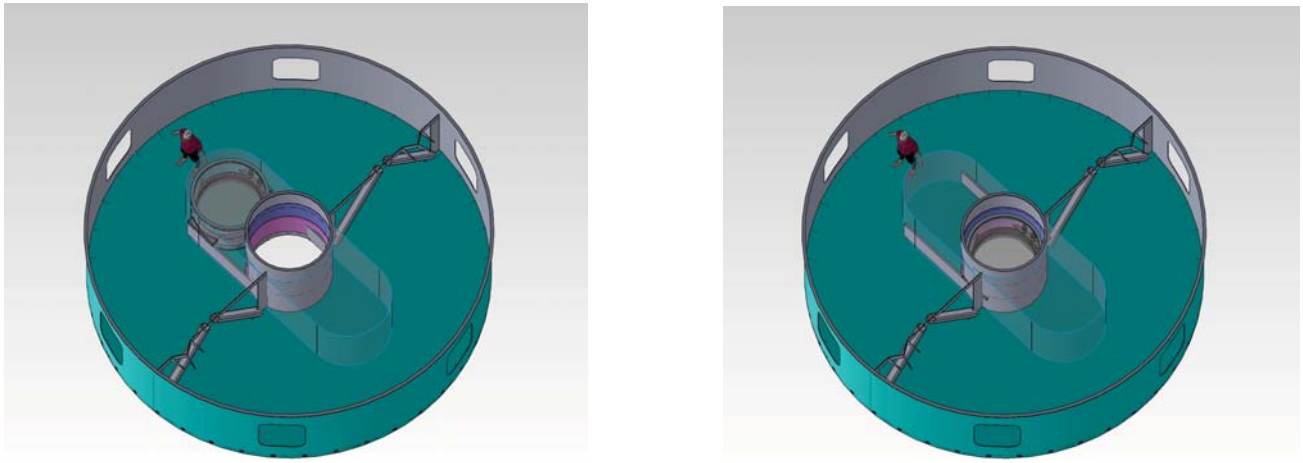

Figure 13. Corrector-ADC in its parked (left) and deployed (right) positions within the central M1 cell structure.

When parked, the corrector-ADC resides in a protective enclosure. The deployed and parked positions are oriented along an axis parallel to the elevation axis, so motion of the subsystem does not change the OSS balance. To accommodate the goal of extended wavelength coverage for the corrector, space has been allocated for the addition of a second corrector element as a future upgrade.

### 6.3 Fast-steering Secondary Mirror Subsystem

A fast-steering secondary mirror subsystem consisting of 7 individual, monolithic segments is provided as a backup to the adaptive secondary mirror subsystem. Each segment consists of a lightweighted, 120mm thick Zerodur blank, supported by 3 actuators that provide fast tip and tilt motion, a vacuum support system to react the normal component of gravity and a central flexure for lateral shear restraint. A seismic restraint system is also provided. A detailed description of the design and development of the fast-steering secondary mirror subsystem is presented by Cho[6].

### 6.4 Secondary Mirror Positioning Subsystem

The M2 positioner is used to support and position the adaptive secondary mirror (ASM) and the fast-steering secondary mirror (FSM) assemblies and provides translation and rotation of the secondary mirror segments to compensate for the slowly changing errors associated with structural deflection due to temperature and elevation changes. The positioner actuators act as a hexapod to enable motion of the secondary mirror segments in 6 degrees of freedom. The preliminary design of these actuators has them nested within the structure of the secondary frame. This mounting arrangement minimizes the offset of the mass of the secondary mirror assembly from the frame and thus improves its dynamic performance. A sketch of the top frame, M2 positioner and FSM secondary mirror segments is shown in Figure 14, below.

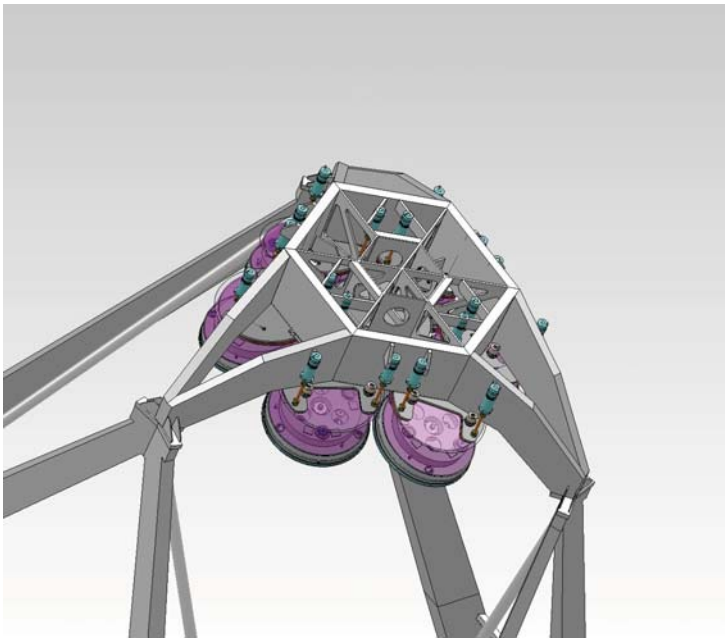

Figure 14. Top frame with M2 positioner actuators and fast-steering secondary mirror segment subassemblies

### 6.5 Acquisition, Guide and Wavefront Subsystem (AGWS)

The acquisition, guide and wavefront subsystem (AGWS) includes acquisition/guide sensors, wavefront sensors and their associated optics and mechanisms (probe assemblies) for deployment into the direct Gregorian beam. These sensors provide information to control of a set of image quality compensators, such as rigid body motions of primary and secondary mirror segments and figure of the primary mirror segments. The deployable probes will pick off the light from stars within the technical field of view (nominally between the 10 and 20 arcmin diameters). The AGWS will

rotate with the GIR and may include components of the adaptive optics system (see Bouchez[5]). A minimum of 3AGWS probe assemblies will be used to patrol the technical field of view.

# 7. MECHANICAL SUBSYSTEMS

## 7.1 Main Axes Drives

The main axes drives provide force, sufficient to move the telescope about its main axes such that point to point motion/time requirements are met. They must also provide stable forces that do not adversely affect dynamic performance of the telescope during science observations. Our preferred drives solution is the use of linear motors. The Center for Electro-Mechanics at the University of Texas at Austin is conducting a preliminary design of the main axes drives using linear motors to assess the feasibility and cost of such a system for the GMT.



Motion requirements dictate a minimum acceleration about each axis of 0.1 degrees per second squared. This, coupled with friction and dynamic disturbance forces requires that the available torque for the elevation axis be not less than 210 kN-m. For the azimuth axis, the minimum available torque must be 285 kN-m. For adequate dynamic performance, force errors must be less than 1% of the peak forces.

Our preliminary design has the magnet tracks attached to the C-rings for the elevation axis drives and on the azimuth track for the azimuth drives. Multiple, fixed forcer heads are attached to the azimuth disk. Four forcer heads, used to move the OSS are located between the OSS radial HBS pads at the top of the four azimuth disk pedestals. Four additional forcer heads, used to move the azimuth disk are located between the azimuth vertical HBS pads.

## 7.2 Hydrostatic Bearing System (HBS)

Hydrostatic bearings provide low friction sliding surfaces for the elevation and azimuth axes at the interfaces between the OSS and the azimuth disk and between the azimuth disk and the azimuth track. Vertical, fore/aft and lateral restraint for the OSS is provided by groups of OSS radial and lateral bearings that bear on and the C-ring runner bearing surfaces at 4 locations. Each bearing group consists of 4 radial bearings, oriented toward the elevation axis and 2 lateral bearings, one on the inside and one on the outside of the C-ring. The radial bearings are configured with master and slave bearing sets where the master bearing directly reacts the load it sees within the bearing group and the slave bearings are fed by a constant pressure supply and therefore see the same load all the time. Vertical and lateral restraint of the azimuth disk is provided by 4 groups of azimuth bearings that bear against the azimuth track runner bearing surfaces. Each bearing group consists of 4 vertical bearings configured with master and slave bearings sets. Each group also has a pair of lateral bearings that bear up against the inside face of the azimuth track. A top down view of the azimuth disk showing the OSS HBS pads is shown in Figure 15.

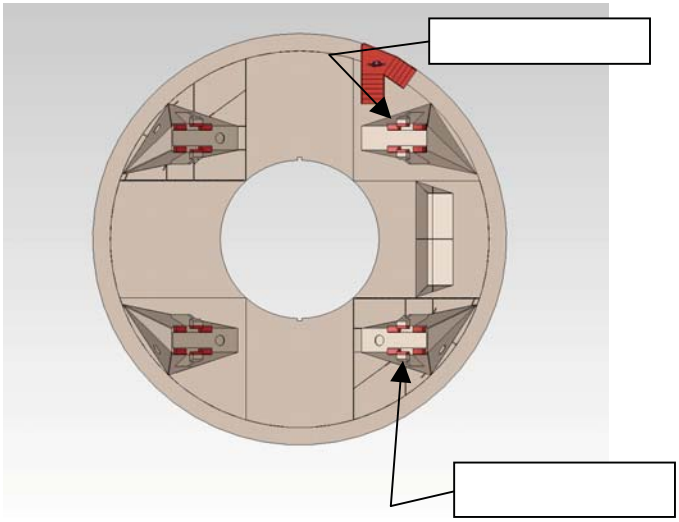

Figure 15. Plan view of the azimuth disk showing the locations of the OSS radial and lateral hydrostatic bearings

To enhance dynamic performance of the telescope, high frequency over-constraint features (HFOC) are employed for each slave bearing. HFOC and its application to GMT dynamic performance are discussed in detail in a paper by Gunnels[1]. HFOC enables slave bearings to retain high axial stiffness under dynamic loading at frequencies greater than about 2 hz, yet exhibit no axial stiffness under the low frequency perturbations. This feature improves the dynamic performance of the telescope when disturbed by forces such as wind or mechanical vibration, but allows the telescope to accommodate irregularities in runner bearing surfaces by enabling the slave bearings to displace axially without change in the forces that they react.

Oil at sufficient pressure and flow rate are supplied to the HBS pads from the hydraulic pumping system through the rigid pipe, hoses and manifolds of the oil supply system. An oil-line transfer system is used to route the oil through the interface between the rotating azimuth disk assembly and the fixed telescope pier. Oil is returned to the pumping system through the oil collection system. The hydraulic oil temperature must be controlled such that the delivered oil temperature to the bearing pads is at a specified temperature relative to the ambient. The hydraulic cooling system provides temperature control of the hydraulic oil.

An ongoing preliminary design study by Tomelleri S.r.l. is being conducted to assess the feasibility and cost of various HBS design configurations for the GMT.

## ACKNOWLEDGEMENTS

This work has been supported by the GMTO Corporation, a non-profit organization operated on behalf of an international consortium of universities and institutions: Astronomy Australia Ltd, the Australian National University, the Carnegie Institution for Science, Harvard University, the Korea Astronomy and Space Science Institute, the Smithsonian Institution, The University of Texas at Austin, Texas A&M University, University of Arizona and University of Chicago.

This material is based in part upon work supported by AURA through the National Science Foundation under Scientific Program Order No. 10 as issued for support of the Giant Segmented Mirror Telescope for the United States Astronomical Community, in accordance with Proposal No. AST-0443999 submitted by AURA.

## REFERENCES

[1] Gunnels, S., "The Giant Magellan Telescope (GMT) - Hydrostatic Constraints", Proc. SPIE 7733, (2010).
[2] Gunnels, S., Kan, S., Sarawit, A., "The Giant Magellan Telescope (GMT) - structure design update", Proc. SPIE 7012, (2008).
[3] Gunnels, S., Davison, W., Cuerden, B., Hertz, E., "The Giant Magellan Telescope (GMT) Structure", Proc. SPIE 5495, (2004).
[4] Johns M., McCarthy, P. J., Raybould, K., Bouchez, A., Farahani, A., Filgueira, J. M., Jacoby, G., Shectman, S., Sheehan, M., "Giant Magellan Telescope: overview (Invited Paper)," Proc. SPIE 8444, (2012).
[5] Bouchez, A., Acton, D.S., Bennet, F. H., Brusa-Zappellini, G., Codona, J. L., Conan, R., Connors, T., Durney, O., Espeland, B.,Gauron, T. M., Lloyd-Hart, M., Hinz, P. M., Kanneganti, S., Kibblewhite, E. J., Knox, R. P., McLeod, B. A., McMahon, T., Montoya, M., Norton, T. J., Ordway, M. P., Parcell, S., Piatrou, P. K., Price, I., Roll, Jr., J. B., Trancho, G., Uhlendorf, K., et al, "The Giant Magellan Telescope Adaptive Optics program", Proc. SPIE 8447, (2012).
[6] Cho, M. K., Corredor, A., Dribusch, C., Park, W. H., Sheehan, M., Johns, M., Shectman, S., Kern, J., Kim, Y. S., "Performance Prediction of a Fast Steering Secondary Mirror for the Giant Magellan Telescope," Proc. SPIE 8444, (2012)
[7] Glaese, R. M., Michael Sheehan, M., "Vibration mitigation for wind-induced jitter for the Giant Magellan Telescope," Proc. SPIE 8444, (2012).
[8] Kan, F.W.,Egers, D.W.,"Wind Vibration Analysis of the Giant Magellan Telescope,"Proc. SPIE 6271, (2006)